The EMBO Journal (2008) 27, 224–233 | © 2008 European Molecular Biology Organization | Some Rights Reserved 0261-4189/08
www.embojournal.org

THE EMBO JOURNAL

EMBO open

Lipids revert inert Aβ amyloid fibrils to neurotoxic protofibrils that affect learning in mice

Ivo Cristiano Martins[1,5], Inna Kuperstein[2,5], Hannah Wilkinson[1], Elke Maes[2], Mieke Vanbrabant[2], Wim Jonckheere[1], Patrick Van Gelder[3], Dieter Hartmann[2], Rudi D'Hooge[4], Bart De Strooper[2,*], Joost Schymkowitz[1,*] and Frederic Rousseau[1,*]

[1]Switch Laboratory, Flanders Institute for Biotechnology (VIB) and Vrije Universiteit Brussel (VUB), Brussel, Belgium, [2]Laboratory for Neuronal Cell Biology and Gene Transfer, Center for Human Genetics, Flanders Institute for Biotechnology (VIB) and KULeuven, Leuven, Belgium, [3]ULTR Laboratory, Department for Molecular and Cellular Interactions, Flanders Institute for Biotechnology (VIB) and Vrije Universiteit Brussel (VUB), Brussel, Belgium and [4]Laboratory of Biological Psychology, KULeuven, Leuven, Belgium

Although soluble oligomeric and protofibrillar assemblies of Aβ-amyloid peptide cause synaptotoxicity and potentially contribute to Alzheimer's disease (AD), the role of mature Aβ-fibrils in the amyloid plaques remains controversial. A widely held view in the field suggests that the fibrillization reaction proceeds 'forward' in a near-irreversible manner from the monomeric Aβ peptide through toxic protofibrillar intermediates, which subsequently mature into biologically inert amyloid fibrils that are found in plaques. Here, we show that natural lipids destabilize and rapidly resolubilize mature Aβ amyloid fibers. Interestingly, the equilibrium is not reversed toward monomeric Aβ but rather toward soluble amyloid protofibrils. We characterized these 'backward' Aβ protofibrils generated from mature Aβ fibers and compared them with previously identified 'forward' Aβ protofibrils obtained from the aggregation of fresh Aβ monomers. We find that backward protofibrils are biochemically and biophysically very similar to forward protofibrils: they consist of a wide range of molecular masses, are toxic to primary neurons and cause memory impairment and tau phosphorylation in mouse. In addition, they diffuse rapidly through the brain into areas relevant to AD. Our findings imply that amyloid plaques are potentially major sources of soluble toxic Aβ-aggregates that could readily be activated by exposure to biological lipids.

The EMBO Journal (2008) **27,** 224–233. doi:10.1038/sj.emboj.7601953; Published online 6 December 2007
Subject Categories: molecular biology of disease; structural biology
Keywords: Alzheimer's disease; amyloid fibril; amyloidosis; lipid

Introduction

Alzheimer's disease (AD) is a neurodegenerative disorder characterized by neurofibrillary tangles and amyloid plaques consisting of aggregated Aβ-peptide (Hardy, 2002). Fifteen years ago, the 'amyloid hypothesis' for AD has been proposed (Selkoe, 1991; Hardy and Higgins, 1992), but the discrepancies between amyloid plaque load in the brain and cognitive impairment in the patient (Price and Morris, 1999) or mice (Games *et al*, 1995) have caused a lot of controversy in the field (Terry, 2001). This has led to the concept of 'protofibrils' (Harper *et al*, 1997; Walsh *et al*, 1997, 1999; Hartley *et al*, 1999), 'annular assemblies' (Lashuel *et al*, 2002; Bitan *et al*, 2003); 'Aβ-derived diffusible ligands' (Lambert *et al*, 1998) or 'soluble toxic oligomers' (Podlisny *et al*, 1995, 1998; McLean *et al*, 1999; Walsh *et al*, 2002a; Glabe and Kayed, 2006). These species are intermediary forms between free soluble Aβ-peptides and insoluble amyloid fibers and are toxic *in vitro* and *in vivo*, whereas mature Aβ-amyloid fibers are largely inert (Aksenov *et al*, 1996). The molecular nature of these smaller assemblies of Aβ remains rather elusive (Hepler *et al*, 2006), as different sources, isolation procedures and biophysical techniques lead to different conclusions. A number of species have been observed: dimeric and trimeric Aβ-oligomers (Podlisny *et al*, 1995, 1998; McLean *et al*, 1999; Walsh *et al*, 2002a), 56* kDa oligomer assemblies from transgenic mouse brains (Lesne *et al*, 2006) or larger structures that consist of 50 and more Aβ peptides (Lambert *et al*, 1998; Walsh *et al*, 1999; Nilsberth *et al*, 2001; Chong *et al*, 2003; Barghorn *et al*, 2005; Wogulis *et al*, 2005; Hepler *et al*, 2006; Haass and Selkoe, 2007).

A β-Amyloid fibrils, on the other hand, are found in the amyloid plaques as large insoluble macromolecular assemblies characterized by a 'cross-β' fiber-like architecture. Mature fibrils are resistant to proteolytic cleavage, are unaffected by denaturant concentrations that unfold globular proteins and possess high thermostability (Booth *et al*, 1997; O'Nuallain *et al*, 2005). Amyloid fibrils from different proteins are biologically inert, although cytotoxicity appears primarily caused by soluble prefibrillar oligomers (Bucciantini

*Corresponding authors. B De Strooper, Laboratory for Neuronal Cell Biology and Gene Transfer, Center for Human Genetics, Flanders Institute for Biotechnology (VIB) and KULeuven, Herestraat 49, Leuven, Belgium. Tel.: +3216346227; Fax: +3216347181;
E-mail: bart.destrooper@med.kuleuven.be or J Schymkowitz or F Rousseau, Switch Laboratory, Flanders Institute for Biotechnology (VIB) and Vrije Universiteit Brussel (VUB), Pleinlaan 2, Brussel 1050, Belgium. Tel.: +3226291425; Fax: +3226291963;
E-mails: joost.schymkowitz@vub.ac.be or frederic.rousseau@vub.ac.be
[5]These authors contributed equally to this work

Received: 14 July 2007; accepted: 19 November 2007; published online: 6 December 2007

et al, 2002). Taken together, these observations suggest an archetypal model for amyloid-associated pathologies in which disease is caused by transient toxic aggregates that eventually convert to inert amyloid deposits. These deposits would then be simple remnants of the aggregation process playing no significant role in the disease process (Lomas *et al*, 1992). On the other hand, amyloid fibrils are not strictly irreversible but rather in a slow dynamic equilibrium with soluble peptide (Carulla *et al*, 2005; O'Nuallain *et al*, 2005). For instance, amyloid fibrils from the PI3 kinase-SH3 domain recycle about half of their molecules over a period of weeks (Carulla *et al*, 2005). Inspired by the fact that disturbed lipid metabolism is increasingly considered as an important factor in AD pathogenesis, we have investigated the influence of biological lipids on the stability of amyloid fibrils of the Alzheimer's β-peptide 1–42 (Aβ42) in relation to neurodegeneration. We focused on sphingolipids (SM) and gangliosides (GM), which are associated with amyloid deposits (Kakio *et al*, 2002; Devanathan *et al*, 2006). In addition, lipid raft domains containing cholesterol (CH), SM and GM promote Aβ aggregation and oligomer formation (Kakio *et al*, 2002; Yip *et al*, 2002; Zou *et al*, 2003; Gellermann *et al*, 2005; Kim *et al*, 2006). Peroxidized lipids and their derivatives such as 4-hydroxynonenal are involved in amyloid aggregation linking oxidative stress to Aβ deposition (IrmingerFinger *et al*, 1999). Finally, phospholipids stabilize toxic oligomers generated from monomeric Aβ (Johansson *et al*, 2007).

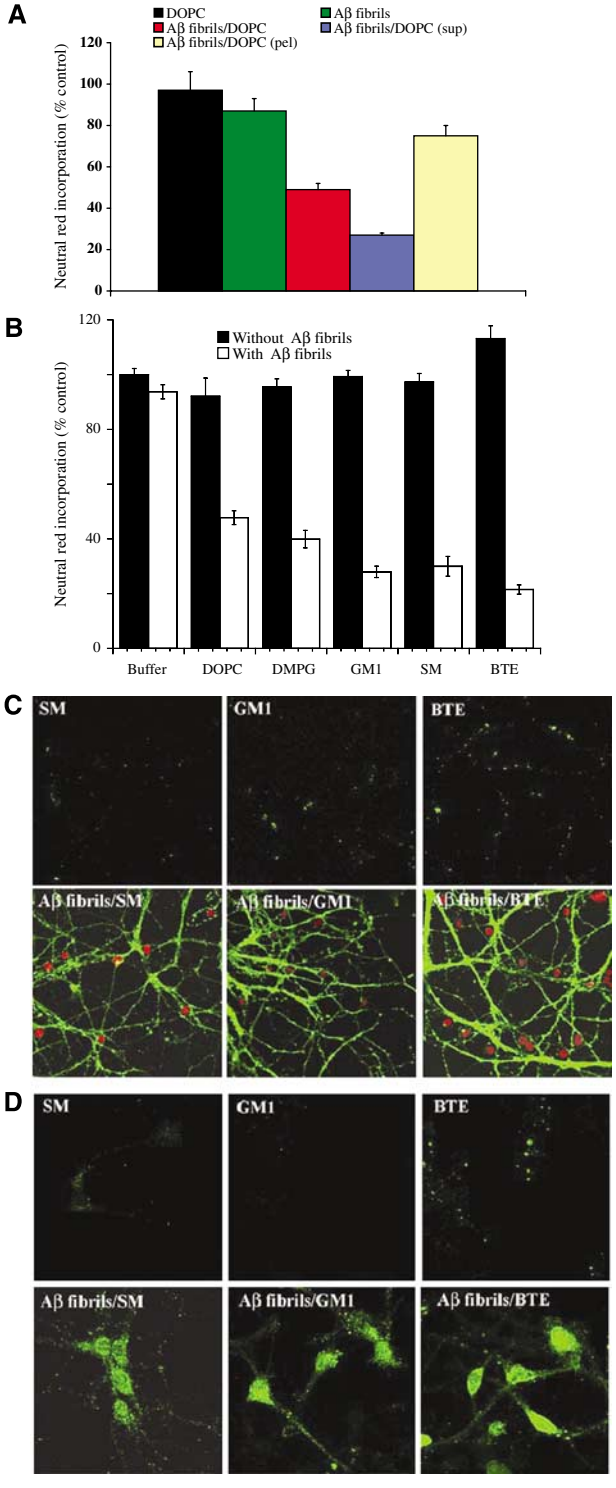

Results

Lipids convert inert amyloid fibrils to a highly toxic species

We measured the effect of lipids on mature amyloid fibrils of Aβ42, in terms of their toxicity to primary neurons *in vitro*. We incubated Aβ42 for 2 weeks at 25°C, at 1 mg ml^{-1} in 50 mM Tris-HCl, pH 7.4, and 5 mM EDTA and controlled the presence of Aβ42 fibrils by electron microscopy. These mature Aβ42 fibrils were subsequently harvested by centrifugation and added to primary hippocampal mouse neurons

Figure 1 Lipid-derived Aβ protofibrils cause neurotoxicity and cell death in primary hippocampal neurons. Inert Aβ fibrils (250 mg ml^{-1}, 50 μM) were incubated with DOPC liposomes (2.5 mg ml^{-1}) overnight while shaking and subsequently added in a 1:10 dilution (5 μM and 0.25 mg ml^{-1} final concentrations of fibrils and lipids, respectively) to primary cultures of hippocampal neurons cultured for 18 DIV (days *in vitro*). (**A**) Neutral red incorporation by neurons after treatment with lipids (0.25 mg ml^{-1} final concentration), Aβ fibrils (5 μM final concentration) or lipid/Aβ fibrils during 48 h was assayed. DOPC liposomes alone (black), Aβ fibrils alone (green), Aβ fibril/DOPC (red), Aβfibril/DOPC soluble fraction obtained by extensive centrifugation (blue) or resuspended Aβfibril/DOPC insoluble pelleted fraction (yellow) are shown. Values are % of control ± s.e.m., $P<0.002$, of three independent experiments performed in triplicate. (**B**) Neutral red incorporation by neurons treated for 24 h with various lipid mixtures (black) or with soluble fraction from Aβ fibril/lipid mixtures (white) is shown (concentrations as above). DOPC, dioleyl phosphatidylcholine; DMPG, dioleyl phosphatidylglycerol, GM1, ganglioside; SM, sphingomyelin (SM); BTE, brain total extract. Values are % of control ± s.e.m., $P<0.006$, of three independent experiments performed in triplicate. Aβ fibrils (5 μM final concentration) or lipid mixtures (0.25 mg ml^{-1} final concentration) alone had no effect on neutral red incorporation. (**C**) AnnexinV/propidium iodide (PI) staining of primary neurons. Fluorescence microscopy images of Annexin V (green) and PI (red) staining of hippocampal neurons cultured for 18 DIV treated with GM1, SM and BTE liposomes and the soluble fraction of the same Aβ fibrils/lipid mixtures in the concentrations mentioned above are shown. Incubation with 5 μM of Aβ fibrils alone did not affect this staining (not shown). (**D**) Cleaved caspase-3 staining. Fluorescence microscopy images of cleaved caspase-3 staining of hippocampal neurons cultured for 18 DIV treated with SM, GM1 and BTE liposomes and soluble fractions of Aβ fibrils/lipid mixtures as mentioned above are shown. Incubation with 5 μM of Aβ fibrils alone did not affect this staining (not shown). Results reveal apoptotic cell death induced by soluble fractions of Aβ fibrils/lipid mixtures but not by Aβ fibrils or lipids alone.

Table I Comparison of the toxicity of SEC fractions of Aβ42 mixed with various lipids

Lipid	Fraction	Neutral red	A11 binding
DMPG	16.9	53.0±6.2	+ +
Cholesterol	16.9	50.5±3.5	+ + +
SM	16.9	43.1±2.4	+ + +
GM1	16.9	36.1±2.9	+ + +
BTE	16.9	25.2±4.3	+ + +

Inert Aβ fibrils (250 mg ml^{-1}, 50 μM) were incubated with liposomes enriched in different lipids (left column in the table) (2.5 mg ml^{-1}) overnight while shaking and then centrifuged as indicated previously. The SEC fractionation of the soluble part of Aβ42 fibril/lipid mixtures shows a peak at 16.9 ml. Toxicity of the 16.9 ml peak from the various Aβ42 fibril/lipid emulsions is quantified by neutral red incorporation into hippocampal neuronal cells. A qualitative indication of binding to the oligomer-specific A11 antibody to the 16.9 ml peak from the various Aβ42 fibril/lipid emulsions detected by dot blot is also given.

at a final concentration of 25 μg ml^{-1} (5 μM). As expected, these mature fibers were largely inert, displaying only modest neurotoxicity as assayed by Neutral Red incorporation. However, an overnight incubation at room temperature of 250 μg ml^{-1} mature Aβ42 fibrils with a 2.5 mg ml^{-1} liposome suspension composed of synthetic lipid dioleyl phosphatidylcholine (DOPC) yielded a toxic emulsion when added to primary hippocampal neurons at a final concentration of 5 μM Aβ peptide fibril and 0.25 mg ml^{-1} lipid (Figure 1A). Importantly, neither lipid preparations (0.25 mg ml^{-1}) nor mature amyloid fibrils (5 μM) alone were toxic (Figure 1A). The toxic Aβ42 fibril/lipid emulsion became partitioned into two phases that were separated by centrifugation for 20 min at 14 000 *g*. The supernatant fraction exhibited a high degree of toxicity, whereas the pellet was largely inert (Figure 1A). Similar lipid-induced neurotoxicity of mature Aβ42 amyloid fibrils was also observed with various other synthetic and membrane lipids, including the gangliosides GM1, sphingomyelin (SM) and brain total lipid extract (BTE) from cow (Table I). Neurotoxicity of the supernatants from these preparations was evaluated in primary cultures of neurons by neutral red incorporation (Figure 1B). The supernatants induced apoptosis, as shown by Annexin V/propidium iodide staining (Figure 1C) and cleaved caspase-3 staining (Figure 1D). Collectively these data strongly suggest that biological relevant lipids, including lipid extracts from brain, can induce the reversal of mature amyloid fibril to a soluble toxic species.

Lipids cause mature amyloid fibrils to disassemble into a protofibrillar species

To determine the mechanism by which lipids cause the conversion of inert amyloid fibrils into a toxic state, we proceeded to the biophysical characterization of fibril–lipid mixtures. As is clear from the introduction, the atypical behavior of Aβ42 in a number of biophysical techniques has led to conflicting interpretations about the nature of the toxic species (Hepler *et al*, 2006). For this reason, we combine a range of biophysical assays, to obtain a maximum of information on the nature of the toxic species we here obtained. Transmission electron microscopy revealed that amyloid fibrils (Figure 2A) were converted by lipids to an insoluble fraction containing fractured and highly intertwined amyloid material surrounded by short amyloid fragments (Figure 2B), whereas the supernatant contained protofibrillar structures (Figure 2C), confirming fibril destablization and resolubilization in the presence of lipids. Confocal microscopy using immunostaining with the antibody A11 that is specific for 'soluble prefibrillar oligomers' (Kayed *et al*, 2003) shows not only a granular decoration of material on the plasma membrane of primary neurons, but also significant internalization (Figure 2D) matching the behavior of prefibrillar toxic material extracted from AD brains (Chromy *et al*, 2003). Amyloid–lipid emulsions were further deposited under a sucrose gradient and centrifuged at 100 000 *g* for 1 h. We used the Aβ-specific mAb 6E10 and the oligomer-specific pAB A11 to detect Aβ species. Although both the top of the gradient and the pellet reacted with 6E10, only the top of the gradient reacted with A11 (Figure 2E), demonstrating that fibrils are indeed resolubilized and that the soluble fraction migrates in the same fraction as the liposomes, whereas insoluble amyloid material was pelleted. Dynamic light scattering (DLS) at a detection angle of 90° relative to the incident beam detected hydrodynamic radii between 10 and 100 μm in samples of mature fibrils (Figure 3A1). When lipids were added to the sample (Figure 3A2), the hydrodynamic radius dropped to a range between 100 nm and 1 μm, indicating significant heterogeneity. A sample of lipids alone was monodispersed with an apparent radius of roughly 200 nm (Figure 3A3). A similar size distribution is observed from light scattering measured at 173° (back scattering), excluding misinterpretations due to the angular dependence of light scattering (data not shown). Both the size distribution and heterogeneity observed by light scattering are in excellent agreement with sizes observed by electron microscopy, where flexible protofibrils are observed to curl into spheroid shapes with dimensions between 100 and 300 nm (Figure 2C). Further confirmation that the amyloid fibrils revert to a protofibrillar state (Walsh *et al*, 1997; Hartley *et al*, 1999) was obtained from spectroscopic analysis, which showed intermolecular β or cross-β structure similar to that of mature amyloid fibrils (Figure 3B and C). Circular dichroism (CD) revealed an increase in the amplitude around 220 nm, but no significant shape change compared to the amyloid far UV spectrum, indicating an increase in soluble material in the amyloid–lipid mixtures with a similar β-sheet content as the amyloid fibrils (Figure 3B). Fourier-transform infrared (FTIR) spectra indicated that lipid-induced protofibrils possess a similar intermolecular β-extended structure as mature fibrils (corresponding to the spectral band at 1623 cm^{-1}), but the difference FTIR spectrum revealed some degree of unfolding in the protofibrils as compared to the mature amyloid fibrils, as was apparent from the 1647 cm^{-1} band (Figure 3C). We proceeded to analyze our lipid-induced protofibrils by size exclusion chromatography (SEC). When the supernatant of a lipid/fibril mixture was injected on an S75/HR10 column, a single peak at 15.8 ml was eluted (Figure 3D, green line), which immunostained with both the 6E10 and A11 antibodies (Figure 3D). Size determination from the elution volume yields an apparent molecular weight of approximately 9 kDa (dimeric Aβ). This estimation, however, is only valid for globular proteins that do not interact with the column matrix. These requirements are certainly not met here, as the analysis of the elution peak

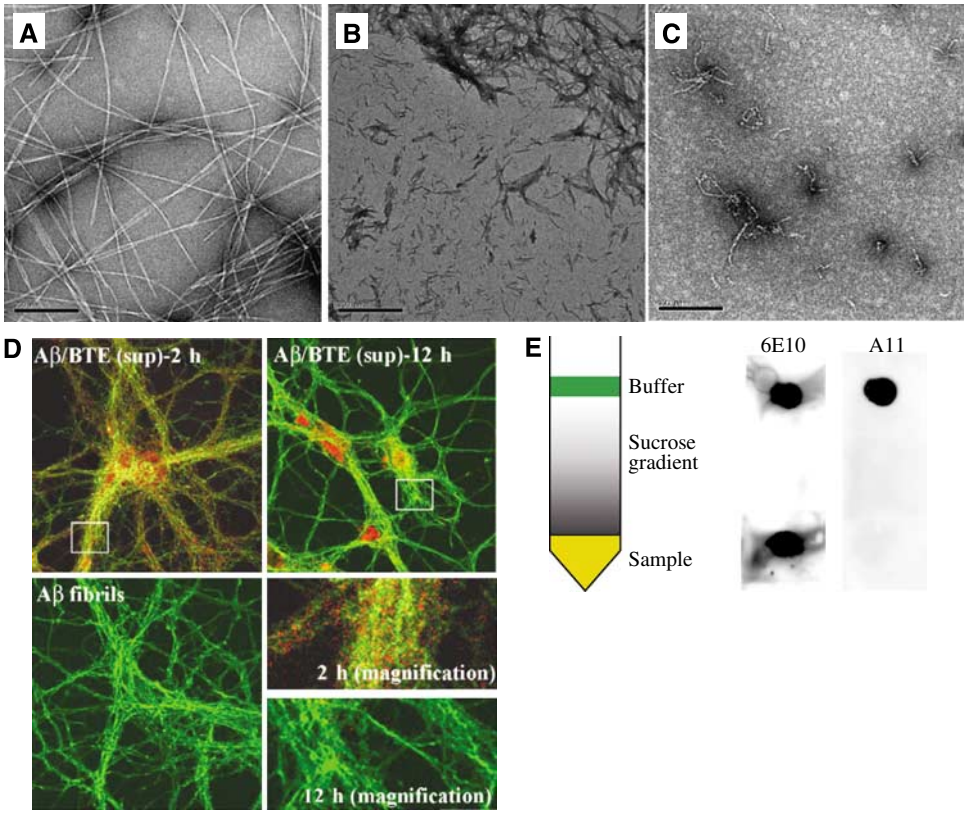

Figure 2 Lipids induce disassembly of mature Aβ42 amyloid fibrils into soluble protofibrils. (**A**) Electron microscopy images showing mature Aβ42 amyloid fibrils alone. (**B**) Aβ42 amyloid fibrils were mixed with DOPC liposomes and the pellet was harvested using centrifugation; the electron micrograph reveal strongly intertwined lipids and amyloid fibrils as well as fragmented amyloid material. (**C**) Electron micrograph of the soluble fraction of the previous image, which contains small oligomeric fragments. The black bar on images A, B and C indicates a size of 200 nm. (**D**) Protofibrils detection by oligomer-specific A11 antibody. Soluble fractions from Aβ fibrils/BTE mixtures display decorating punctuate-like hippocampal neurons staining detected by the oligomer-specific A11 antibody (red) versus actin staining (green) revealing binding of oligomers to the cell surface and intracellular localization at later time points. (**E**) 'Floating assay' by ultracentrifugation reveals Alzheimer's Aβ42 oligomers in association with liposomes in amyloid/lipid mixtures (250 μg ml^{-1} peptide, 2.5 mg ml^{-1} lipid). After centrifugation for 1 h at 150 000 *g*, liposomes are in the top fraction, whereas protein aggregates are expected in the pellet. As 6E10 immunostaining indicates, some Aβ42 material is indeed removed to the pellet, but a significant amount is transported to the top fraction in association with the lipids. This fraction is equally recognized by the oligomer-specific antibody A11, consistent with fibril disassembly, whereas the pellet fraction is not recognized by A11 and most likely contains intact fibrils.

by TEM again clearly shows a heterogeneous mixture of protofibrillar oligomers with a size of 100–200 nm. To characterize the size distribution of the lipid/fibril mixture, we instead utilized an 18-angles static light scattering (SLS) detector inline with the SEC column, which allows to infer size information directly from the angular dependence of the scattered light intensity in an absolute manner that is independent from shape or gel matrix interactions. SLS indicates a strong nonlinear angle dependence in the light scattering intensity (Figure 3E), consistent with objects larger than 100 nm, and calculated molecular weights of 80–500 kDa (between 20 and 90 monomeric units). The fact that a heterogeneous sample elutes as a focused peak is consistent with strong interactions with the gel matrix, as under these conditions the elution profile is no longer determined by the size but by the strength of the column interactions and no size separation is achieved. Taken together, the methods used here are in agreement with earlier analysis of the structure (Walsh *et al*, 1999; Hepler *et al*, 2006) and toxicity (Walsh *et al*, 1997, 2002b) of protofibrils and indicate that the sample cannot be defined by a single molecular mass.

'Backward' protofibrils obtained by destabilizing mature fibrils using lipids are identical to 'forward' protofibrils obtained in ageing solutions of monomeric Aβ

We proceeded to compare fibril-derived protofibrils (further termed 'backward' protofibrils) with the extensively studied soluble protofibrils formed during the aggregation process of fresh Aβ (and further termed 'forward' protofibrils). When we incubated monomeric Aβ42 at 1 mg ml^{-1} in 50 mM Tris-HCl, pH 7.4, and 1 mM EDTA at 25°C, we found, consistent with previous observations (Walsh *et al*, 1999; Bitan and Teplow, 2004; Klyubin *et al*, 2005), that neurotoxicity of forward protofibrils peaked between 24 and 48 h (Figure 1F), at which point the sample contains a mixture of protofibrils and some mature fibrils (Figure 4A). Subsequently, the sample becomes inert and highly enriched of mature amyloid fibrils (Figure 2A shows 2-week-old samples) and does not contain detectable amounts of soluble protofibrils anymore. Interestingly, toxicity of forward protofibrils and lipid-induced backward protofibrils is very similar (Figure 4B). Soluble fractions of forward protofibrils

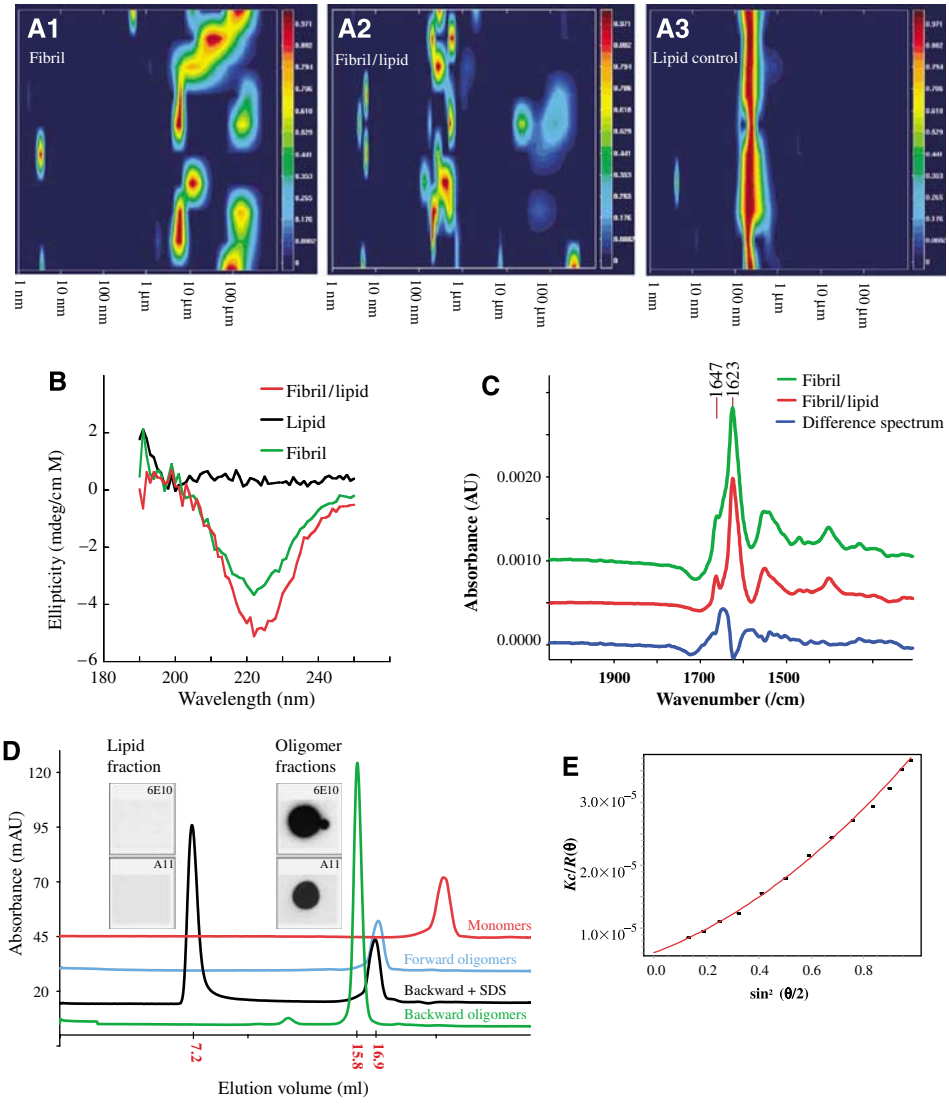

Figure 3 Biophysical characterization of lipid-induced protofibrils. (**A**) DLS spectra of mature Aβ42 fibrils (A1), fibril/lipid mixtures (A2) and pure liposome preparations (A3, DOPC). Apparent hydrodynamic radii are indicated on the *x* axis (logarithmic scale), the *y* axis shows the evolution of the signal during the experiment (20 s) and the color code indicates a relative intensity scale between 0 and 1. The liposome spectrum (A3, 2.5 mg ml^{-1} lipid concentration) reveals strong monodispersity in the sample with an average hydrodynamic radius just above 100 nm, whereas the amyloid fibril sample (A1, 50 μM peptide concentration) contains a wider range of molecular sizes, ranging from 5 to 100 μm approximately. The spectrum of the amyloid–lipid mixture (A2, 50 μM peptide concentration and 2.5 mg ml^{-1} lipid concentration) shows a complete loss of signal for hydrodynamic radii above 5 μm. The majority of the signal shows strong heterogeneity with sizes ranging from 100 nm and 1 μm, consistent with the disassembly of amyloid fibrils into smaller species. (**B**) Far UV CD spectroscopy gives information on the secondary structure of material in solution. The spectra of Aβ42 amyloid fibrils in isolation (50 μM) and in the presence of liposomes (2.5 mg ml^{-1}) containing DMPG display a marked increase in the intensity of the spectrum around 220 nm, while the overall shape of the spectrum is constant. This is consistent with an increase in the amount of soluble material rich in β-sheet content. Similar results were obtained with other lipids (not shown). (**C**) FTIR yields information on the secondary structure of both the soluble and insoluble material in the sample. The spectra of mature Aβ42 fibrils (50 μM) and fibril/lipid mixtures (BTE, 2.5 mg ml^{-1}) show a strong cross-β signal at 1623 cm^{-1}, consistent with a comparable β-sheet content for amyloid fibrils and protofibrils. However, the difference spectrum reveals an additional band at 1647, corresponding to the formation of random coil in the amyloid/lipid mixture, consistent with partial fibril disassembly. (**D**) SEC on a GEHealthcare S75/HR10 column of 'forward' (blue line) and lipid-induced ('backward') oligomers (green line). For each sample, 200 μl of an amyloid–lipid mixture containing 250 μg of Aβ42 peptide and 2.5 mg ml^{-1} lipid were injected. Notice peak elutions at 15.8 ml and 16.9 ml, respectively. Upon 0.1% SDS treatment, backward oligomers elute at the same position as forward oligomers, whereas lipids elute in the void volume (black line). For comparison, an elution trace for monomeric Aβ42 is also shown (red line, elution peak at 21 ml). Elution profiles of amyloid fibril samples show no noticeable peaks. Inset show immunostaining of the lipid fraction and the Aβ42/lipid-induced oligomer fraction of the black profile using the antibody A11, which specifically detects oligomers, and the 6E10 mAb, which is specific for Aβ. (**E**) Eighteen-angles SLS, placed inline with the SEC system, allows to determine molecular mass in an absolute manner that does not depend on interactions with column matrix (as is the case in SEC) or assumed molecular shape (as is the case in DLS). The 15.8 ml peak shown in Figure 3D was analyzed in this manner. The Zimm plot (see Materials and methods) in Figure 3E shows the clear nonlinear dependence of the light scattering intensity with scattering angle, consistent with a radius of gyration larger than 80 nm. The red curve indicates a fit to a quadratic equation (R-squared value >0.9). The molecular masses obtained in this manner vary throughout the peak, in agreement with the heterogeneity observed in DLS and electron microscopy and consistent with a total loss of size-sorting effects from the column due to nonspecific matrix interactions. Masses obtained vary from 80 to 500 kDa throughout the peak.

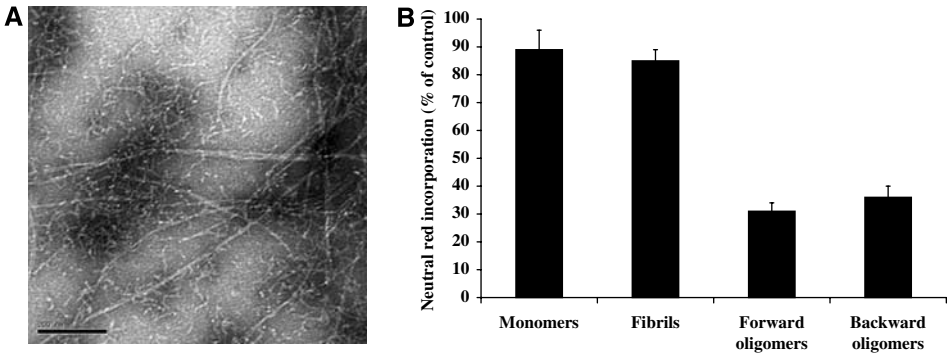

Figure 4 Morphology and toxicity of forward protofibrils. (**A**) Electron micrograph of 48 h aged solution of freshly dissolved Aβ42 reveals a mixture of protofibrillar intermediates and the first appearance of some amyloid fibrils. (**B**) Neutral red incorporation by hippocampal neurons treated with monomers (5 μM), mature Aβ fibrils (5 μM), forward oligomers generated from monomers during 48 h aggregation (5 μM) and soluble fractions of Aβ fibrils/lipid mixtures at 5 μM and 0.25 mg ml^{-1} final concentrations of fibrils and lipids, respectively (termed as 'backward lipid-derived protofibrils', see text). Values are % of control ± s.e.m., $P<0.008$, of two independent experiments performed in quadruplicates.

preparations elute as a single peak at 16.9 ml on an S75/HR10 column (Figure 3D, blue line) and appear as typical protofibrils of 100–200 nm diameter by transmission electron microscopy (Figure 4A). This slight difference in elution volume between the forward protofibrils and backward, lipid-induced protofibrils (15.8 ml) is consistent with an increase in molecular weight due to lipid association. In agreement, upon addition of 0.1% SDS (submicellar concentration) to amyloid–lipid mixtures before injection on the column, a lipid peak eluted in the void volume, whereas the lipid-induced protofibrils now elute at the same elution volume as forward protofibrils (16.9 ml; Figure 3D). These data suggest that, under the incubation condition used here, lipid-induced backward protofibrils have very similar morphological and biochemical properties as the protofibrils formed during the aggregation process of fresh monomers.

In vivo toxicity of backward protofibrils in the brain of adult mice

To further characterize the physiological relevance of the lipid-induced 'backward' oligomers, we proceeded to bilateral intraventricular injection (3 μl) of mature Aβ42 amyloid fibrils, lipids and supernatants from amyloid–lipid mixtures into the brain of adult mice. Immunostaining of brain samples with the 6E10 antibody demonstrated the effective delivery of Aβ in the ventricles when both fibrils and backward oligomers were injected into the animals (Figure 5A). However, within 90 min of injection, we also observed Aβ42 immunoreactivity away from the needle tracks into the cortex (Figure 5A), with oligomeric preparations but not with Aβ fibrils. With the latter, staining remained mostly associated with the ventricular walls (Figure 5A). When we analyzed brain areas further away from the needle track, we observed very little immunostaining after Aβ fibril injections, whereas backward oligomers caused significant staining of the hippocampal areas (Figure 5B), indicating rapid diffusion of (some of) these species into the brain parenchym (Figure 5B). Interestingly, the single injection with backward oligomers caused also mild neurotoxicity restricted to the area of the frontal cortex (but not hippocampus) that was exposed to the highest concentrations of toxic oligomers as revealed by immunostaining for cleaved caspase 3 (Figure 5C) and phosphorylated tau (Figure 5D). Lipid or mature fibrils injection alone did not cause toxicity in the frontal cortex (Figure 5C and D).

Backward and forward protofibrils cause similar memory defects in mouse

To further assess if the lipid-induced 'backward' protofibrils might cause functional deficits relevant to AD, we evaluated the acute biological effects of the injected backward oligomers in exploratory and memory/learning tests. Open-field recording revealed increased path length covered, higher velocity and increased frequencies of center visits, but declined time spent in the center by animals injected with backward oligomers, in sharp contrast to animals injected with lipid samples or mature fibrils alone. As all animals were treated identically, the backward oligomers appear to specifically affect brain functions that cause hyperlocomotion and hyperactivation (Figure 6A). In a light–dark step through task (passive avoidance test), animals were allowed to memorize the electrical shock that follows entrance to a dark compartment. When the test was repeated 24 h later, animals injected with lipids or mature fibrils correctly recalled the electroshock and avoided to enter the dark room. Injection of backward oligomers before the shock event prevented animals from successful memory formation, as was evidenced by uninhibited entering of the dark compartment 24 h after electroshock (Figure 6B). In addition, contextual and auditory-cue fear conditioning showed that injection of backward oligomers 90 min before conditioning severely disturbed typical freezing behavior 24 h later when the animals were exposed again to the same contextual or auditory stimulus, in contrast to the control mice injected with lipids or mature amyloid alone (Figure 6C). One week after oligomer injection, mice appeared to have recovered completely and could no longer be distinguished in open-field activity from control or untreated animals (not shown in figure). Thus, a single injection of lipid-induced backward oligomers appears not to have caused persistent functional defects, which is in excellent agreement with earlier studies of 'forward' oligomers, which were reported to have immediate but transient effects on synaptic function (Wang and Hecht, 2002; Chromy *et al*,

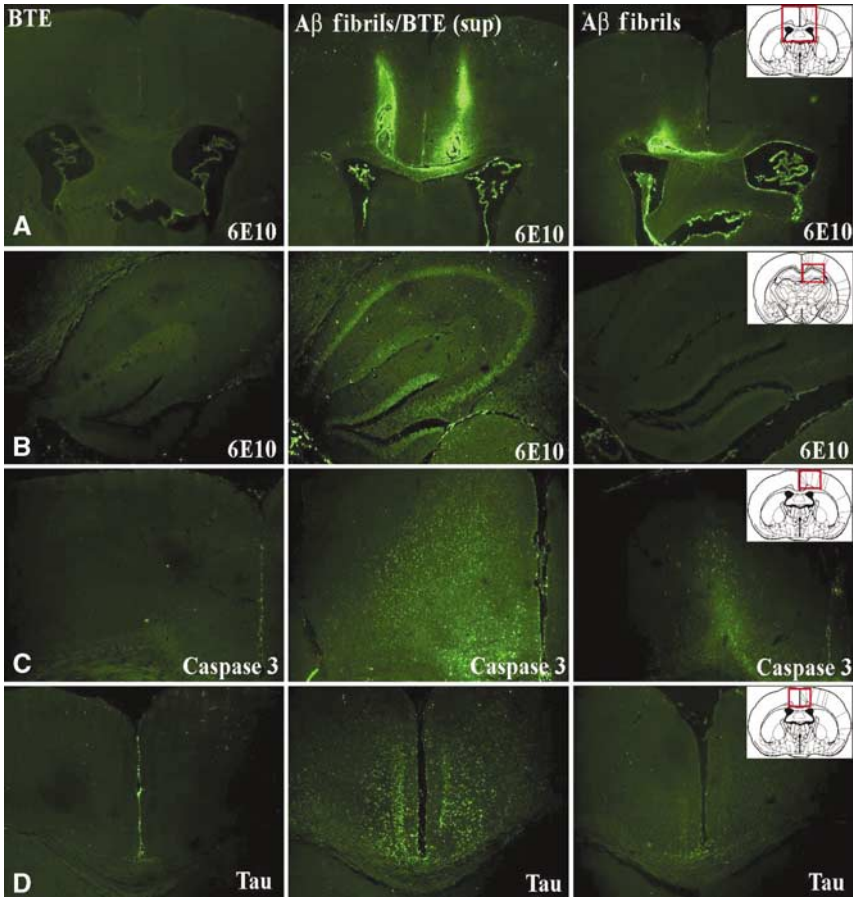

Figure 5 Lipid-derived Aβ protofibrils diffuse rapidly in the brain of mice. (**A**) Detection of intraventricularly injected Aβ preparations in the mouse brain. Inert Aβ fibrils (250 mg ml^{-1}, 50 μM) were incubated with BTE liposomes (2.5 mg ml^{-1}) overnight while shaking and then centrifuged as indicated above. A volume of 3 μl of Aβ fibrils/BTE mixtures soluble fractions from these preparations were injected bilaterally into the lateral ventricles. The same volume of mature fibrils (50 μM) or lipid preparations (2.5 mg ml^{-1}) alone were injected into two control groups. After 1.5 h, mice were killed, and staining with the Aβ-specific mAb 6E10 antibody revealed strongly pronounced Aβ staining along the needle track and in the ventricles in fibrils/BTE mixtures soluble fractions-injected brains (A, middle panel). Similar staining in the ventricles is observed when Aβ fibrils alone are injected, but much less staining is observed along the needle tracks (A, right panel), indicating partial perfusion of soluble Aβ species, but not mature fibrils in the brain tissue. Brains of mice injected with BTE lipid alone did not show Aβ-specific staining (A, left panel). (**B**) Distribution of intraventricularly injected Aβ preparations in the hippocampus of mouse brain. After 1.5 h of injection, strong and specific staining of the hippocampal area is observed with mAb 6E10 when fibrils/BTE mixture-soluble fractions are injected (B, middle panel). Such staining is not observed with lipids (B, left panel) or Aβ fibrils injected alone (A, right panel). (**C**) Cleaved Caspase-3 detection in mouse brain injected with Aβ preparations. Injection of fibrils/BTE mixture-soluble fraction for 24 h caused cleaved caspase-3 (cell signaling) activation in frontal cortex area (C, middle panel). Some caspase-3 staining limited to the area around ventricles and needle track is seen with fibril injections (A, right panel). Such staining is not observed with lipids (B, left panel). (**D**) Phosphorylated tau detection in mouse brain injected with Aβ preparations. Phosphorylated tau staining (AT8 mAb) was detected in the same frontal cortex areas as for cleaved caspase-3 in brains injected with fibrils/BTE mixture-soluble fraction and fibrils. Data indicate that apoptotic markers such as caspase-3 activation and tau phosphorylation are associated with distribution of soluble Aβ in brains injected with fibrils/BTE mixture-soluble fraction, but less in fibrils-injected brains.

2003; Gong *et al*, 2003). Therefore, to directly compare the behavioral effects of forward and backwards protofibrils, we performed identical behavioral tests on animals injected with forward oligomers generated from Aβ42 monomers that were incubated for 48 h at room temperature at a concentration of 1 mg ml^{-1}. These animals showed very similar behavioral defects: open-field recording indicated hyperlocomotion and hyperactivation effects (result not shown) and light–dark step through tests (passive avoidance) showed that animals injected with forward oligomers failed to memorize the electrical shock, in contrast to control individuals injected with buffer (Figure 6D). In addition, contextual and auditory-cue fear conditioning showed that injection of forward oligomers 90 min before conditioning severely disturbed freezing behavior 24 h later, in contrast to the control mice (Figure 6E).

Our results confirm the behavioral effects of forward protofibrils generated from Aβ monomers (Hartley *et al*, 1999; Walsh *et al*, 2002a; Kamenetz *et al*, 2003; Cleary *et al*, 2005; Klyubin *et al*, 2005; Lesne *et al*, 2006; Townsend *et al*, 2006) and show that lipid-induced protofibrils generated from mature Aβ fibrils have very similar pathophysiological effects.

Discussion

We demonstrate in the current work that amyloid fibrils, usually considered as highly stable and biologically inert structures, can be destabilized and easily reverted to soluble and highly toxic Aβ aggregates by biological lipids that are present in the brain. This suggests that part of the critical

A

	General	General	Centre	Centre
	Path length (cm)	Velocity (cm/s)	Visit frequency	Duration (s)
BTE	2469±132	4±0.4	8±1.2	104±10.2
Aβ fibrils/BTE	8151±907	8±0.8	32±3.1	32±3.7
Aβ fibrils	1829±135	3±0.2	6±1.1	166±13

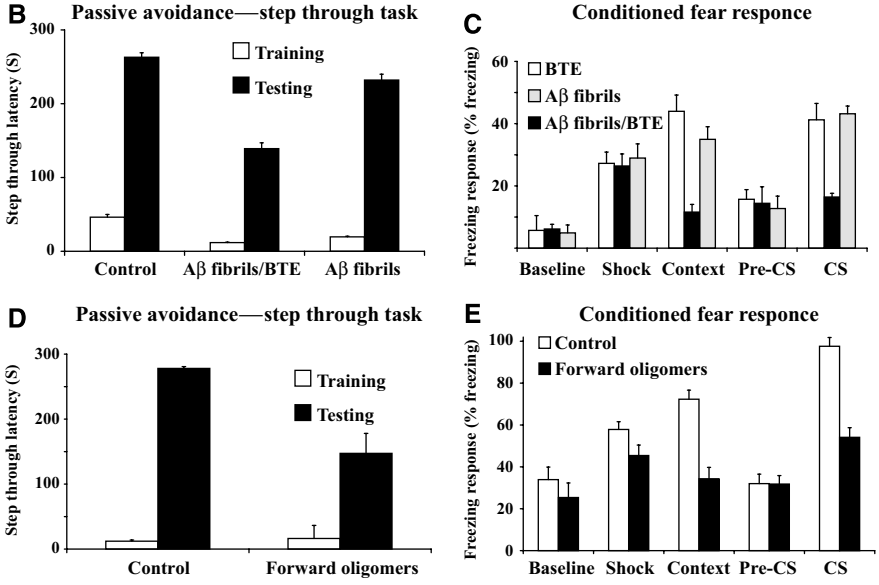

Figure 6 Lipid-derived and forward Aβ protofibrils cause learning and memory impairments in mice. A volume of 3 μl of Aβ fibrils/BTE mixtures soluble fractions, mature fibrils or lipids were injected bilaterally into the lateral ventricles under local anesthesia as indicated in Figure 5. After 1.5 h, mice were evaluated in several behavioral assays. (**A**) Open-field recording of mice injected with backward protofibrils. The table displays total path length covered, velocity, frequencies of center visits and time spent in center. Data reveal that injection of Aβ fibrils/BTE mixture-soluble fractions caused increased velocity and path length covered and increased frequency of visits to the center, but declined time spent in the center. Overall, these indicate hyperactivation and hyperactivity. This effect is not observed in groups injected with mature fibrils and lipids alone (values are mean±s.e.m., $P<0.007$, $n=20$, 21 and 13 for BTE, Aβ fibrils and Aβ fibrils/BTE, respectively). (**B**) Passive avoidance test of mice injected with backward protofibrils. Light–dark step through test showed latency of entrance during the training accompanied with electrical shock (white) and during the testing 24 h later (black). Injection of Aβ fibrils/BTE mixture-soluble fractions 1.5 h before the shock impaired memory in contrast to groups injected with mature fibrils and lipids alone (values are latency mean±s.e.m., $P<0.04$, $n=15$ for each experimental group). (**C**) Contextual fear response test of mice injected with backward protofibrils. Mice groups injected with BTE (white), Aβ fibrils (gray) and Aβ fibrils/BTE mixture-soluble fractions (black) were provided with an electrical stimulus accompanied by an auditory conditioned stimulus 1.5 h after the injection. Memorization of this combination is tested after 24 h by the freezing behavior of the mice exposed to the similar context or to the auditory conditioning stimulus. Data show decreased freezing events (indicating memory disturbances) during exposure to context and to conditioned stimulus in the group injected with Aβ fibrils/BTE mixture-soluble fractions in contrast to groups injected with mature fibrils and lipids alone (values are % freezing mean±s.e.m., $P<0.005$, $n=20$, 21 and 13 for BTE, Aβ fibrils and Aβ fibrils/BTE, respectively). (**D**) Passive avoidance test of mice injected with forward protofibrils. Light–dark step through test showing latency of entrance during the training accompanied with electrical shock (weight) and during the testing 24 h later (black) (values are latency mean±s.e.m., $P<0.001$, $n=10$ for oligomers group and 6 for control group). (**E**) Contextual fear response test of mice injected with forward protofibrils. Freezing response during the test blocks in groups injected with vehicle (weight) and forward Aβ oligomers (black) 1.5 h after the injection (values are % freezing mean±s.e.m., $P<0.005$, $n=12$ for oligomers group and 6 for control group).

balance between toxic and inert Aβ pools is determined by the relative amounts of lipids in the direct environment of the plaques. Remarkably, the toxic species we identify shares many properties with previously characterized 'forward' oligomeric aggregates in terms of biophysical, cell biological and behavioral assays. Although in SEC and other biophysical assays the impression could arise that these structures are homogenous, further extensive biophysical characterization indicates that the size distribution of these oligomeric aggregates is rather heterogeneous in nature, ranging from 80 to 500 kDa, although their morphology is protofibrillar. The appearance of these species indeed varies somewhat with the assay used, likely reflecting their dynamic nature. In that regard, our findings are very similar to the overall picture emerging from the literature and synthesized recently by Hepler *et al* (2006) that also the classical forward oligomeric Aβ structures have to be considered as a spectrum of dynamic structures that are likely in fast equilibrium with each other. Lipids are apparently promoting the equilibrium toward the protofibrillar pools, inducing toxicity of the amyloid mixture. Interestingly our data also confirm that these oligomeric structures diffuse very rapidly throughout the brain and preferentially localize to specific regions of the brain, such as the hippocampus.

Our findings have important implications for the understanding and the treatment of amyloidoses and, in particular, AD. They suggest the possibility that inert amyloid plaques or fibrils could be turned into highly toxic oligomers when local physicochemical parameters are altered due, for instance, to a change in lipid metabolism. Our results could explain why the amount of amyloid deposits and the severity of associated disease symptoms in AD do not necessarily correlate. Individual and temporal differences in brain lipid content could indeed explain why some patients with large amounts

of amyloid deposits display little symptomatic disease, although others are severely affected. In any event, our data strongly suggest that amyloid plaques, although apparently biologically inert, should not be considered as inert remnants of the aggregation process, as the amyloid fibrils they contain can, under certain conditions, be rapidly reverted to toxic species. In that sense, the amyloid plaques should rather be considered as reservoirs of toxicity.

Materials and methods

Chemicals

Alzheimer's β-peptide 1–42 was purchased from Sigma-Aldrich. All purified and synthetic lipids were obtained from Avanti Lipids (USA). Uranyl acetate was obtained from BDH.

Preparation of lipid vesicles and liposomes

All lipids were obtained from Avanti Polar Lipids (USA) except the ganglioside GM1, which was obtained from Larodan Chemicals (Sweden). The stock concentration was 20 mg ml^{-1} in chloroform. The various lipid mixtures discussed in the paper were prepared in Corex round-bottomed glass tubes, dried under a gentle N2 stream and resuspended in 400 μl of diethylether for 10 min at room temperature, after which they were quickly dried in a waterbath at 50°C. The resulting film was placed under vacuum for 1 h to remove trace solvent and rehydrated in 800 μl of 50 mM Tris, pH 7.5, 1 mM EDTA and 0.1 mM NaCl. The resulting vesicle suspension was allowed to stabilize for 1 h at room temperature, sonicated for 15 s (Branson sonifier) and extruded 11 times with an Avanti mini-extruder (Avanti Polar Lipids, USA). This suspension was purified on an S75 gel filtration column using an Akta system from GEHealthcare (UK). The approximate lipid concentration in the stock preparation was 10 mg ml^{-1}. To obtain stable liposomes, it is not possible to use pure preparations of certain lipids such as cholesterol or GM1. Therefore, we used a more complex composition as follows: (i) pure DOPC; (ii) 50% DOPC, 50% DMPG; (iii) 35% DOPC, 35% DMPG, 30% cholesterol; (iv) 30% DOPC, 30% DMPG, 30% cholesterol, 10% GM1; (v) 30% DOPC, 30% DMPG, 30% cholesterol, 10% SM; (vi) 30% DOPC, 30% DMPG, 30% cholesterol, 10% brain total extract.

Preparation of amyloid fibrils, amyloid/lipid mixtures and Aβ oligomers

Amyloid fibrils of the Alzheimer's β-peptide 1–42 were obtained by incubation of 200 μM peptide solution in 50 mM Tris, pH 7.5, for 2 weeks at room temperature. Amyloid fibril/lipid mixtures were prepared by diluting fibril and liposome stock solutions $\frac{1}{4}$ in liposomes buffer and incubating for 1–16 h at room temperature, shaking at 700 r.p.m. Oligomers were generated from monomers by incubation of 200 mM peptide solution in 50 mM Tris, pH 7.5, for 48 h and subsequent extensive centrifugation, and the supernatant as the oligomer-enriched preparation was used immediately. The presence of oligomers in the supernatant was validated by probing with anti-oligomer-specific antibody (A11).

Additional methods can be found in Supplementary data.

Supplementary data

Supplementary data are available at *The EMBO Journal* Online (http://www.embojournal.org).

Acknowledgements

ICM was supported by a PhD scholarship from the Boerhinger Ingelheim Fonds (BIF, Germany), Foundation for Basic Research in Biomedicine, and subsequently a PhD scholarship from the Fundação para a Ciência e Tecnologia (FCT, Portugal), from the Portuguese Ministry for Science and Technology (MCTES). Research in BDS laboratory is supported by a Freedom to Discover grant from Bristol Myers Squib, a Pioneer award from the Alzheimer's Association, the Fund for Scientific Research, Flanders; the Artificial SynApse (IWT-ASAP), KU Leuven (GOA) IUAP P6/43 and a Methusalem grant of the Flemish Government. The VIB Switch laboratory was supported by a grant from the Federal Office for Scientific Affairs, Belgium (IUAP P6/43), and the Fund for Scientific Research, Flanders.

References

Aksenov MY, Aksenova MV, Butterfield DA, Hensley K, Vigo-Pelfrey C, Carney JM (1996) Glutamine synthetase-induced enhancement of beta-amyloid peptide A beta (1–40) neurotoxicity accompanied by abrogation of fibril formation and A beta fragmentation. *J Neurochem* **66:** 2050–2056

Barghorn S, Nimmrich V, Striebinger A, Krantz C, Keller P, Janson B, Bahr M, Schmidt M, Bitner RS, Harlan J, Barlow E, Ebert U, Hillen H (2005) Globular amyloid beta-peptide oligomer—a homogenous and stable neuropathological protein in Alzheimer's disease. *J Neurochem* **95:** 834–847

Bitan G, Teplow DB (2004) Rapid photochemical cross-linking—a new tool for studies of metastable, amyloidogenic protein assemblies. *Acc Chem Res* **37:** 357–364

Bitan G, Vollers SS, Teplow DB (2003) Elucidation of primary structure elements controlling early amyloid beta-protein oligomerization. *J Biol Chem* **278:** 34882–34889

Booth DR, Sunde M, Bellotti V, Robinson CV, Hutchinson WL, Fraser PE, Hawkins PN, Dobson CM, Radford SE, Blake CC, Pepys MB (1997) Instability, unfolding and aggregation of human lysozyme variants underlying amyloid fibrillogenesis. *Nature* **385:** 787–793

Bucciantini M, Giannoni E, Chiti F, Baroni F, Formigli L, Zurdo J, Taddei N, Ramponi G, Dobson CM, Stefani M (2002) Inherent toxicity of aggregates implies a common mechanism for protein misfolding diseases. *Nature* **416:** 507–511

Carulla N, Caddy GL, Hall DR, Zurdo J, Gairi M, Feliz M, Giralt E, Robinson CV, Dobson CM (2005) Molecular recycling within amyloid fibrils. *Nature* **436:** 554–558

Chong YH, Shin YJ, Suh YH (2003) Cyclic AMP inhibition of tumor necrosis factor alpha production induced by amyloidogenic C-terminal peptide of Alzheimer's amyloid precursor protein in macrophages: involvement of multiple intracellular pathways and cyclic AMP response element binding protein. *Mol Pharmacol* **63:** 690–698

Chromy BA, Nowak RJ, Lambert MP, Viola KL, Chang L, Velasco PT, Jones BW, Fernandez SJ, Lacor PN, Horowitz P, Finch CE, Krafft GA, Klein WL (2003) Self-assembly of Abeta(1–42) into globular neurotoxins. *Biochemistry* **42:** 12749–12760

Cleary JP, Walsh DM, Hofmeister JJ, Shankar GM, Kuskowski MA, Selkoe DJ, Ashe KH (2005) Natural oligomers of the amyloid-beta protein specifically disrupt cognitive function. *Nat Neurosci* **8:** 79–84

Devanathan S, Salamon Z, Lindblom G, Grobner G, Tollin G (2006) Effects of sphingomyelin, cholesterol and zinc ions on the binding, insertion and aggregation of the amyloid Abeta(1–40) peptide in solid-supported lipid bilayers. *FEBS J* **273:** 1389–1402

Games D, Adams D, Alessandrini R, Barbour R, Berthelette P, Blackwell C, Carr T, Clemens J, Donaldson T, Gillespie F, Guido T, Hagopian S, Johnson-Wood K, Khan K, Lee M, Leibowitz P, Lieberburg I, Little S, Masliah E, McConlogue L *et al* (1995) Alzheimer-type neuropathology in transgenic mice overexpressing V717F beta-amyloid precursor protein. *Nature* **373:** 523–527

Gellermann GP, Appel TR, Tannert A, Radestock A, Hortschansky P, Schroeckh V, Leisner C, Lutkepohl T, Shtrasburg S, Rocken C, Pras M, Linke RP, Diekmann S, Fandrich M (2005) Raft lipids as common components of human extracellular amyloid fibrils. *Proc Natl Acad Sci USA* **102:** 6297–6302

Glabe CG, Kayed R (2006) Common structure and toxic function of amyloid oligomers implies a common mechanism of pathogenesis. *Neurology* **66:** S74–S78

Gong Y, Chang L, Viola KL, Lacor PN, Lambert MP, Finch CE, Krafft GA, Klein WL (2003) Alzheimer's disease-affected brain: presence of oligomeric A beta ligands (ADDLs) suggests a molecular

basis for reversible memory loss. *Proc Natl Acad Sci USA* **100:** 10417–10422

Haass C, Selkoe DJ (2007) Soluble protein oligomers in neurodegeneration: lessons from the Alzheimer's amyloid beta-peptide. *Nat Rev Mol Cell Biol* **8:** 101–112

Hardy J (2002) Testing times for the 'amyloid cascade hypothesis'. *Neurobiol Aging* **23:** 1073–1074

Hardy JA, Higgins GA (1992) Alzheimer's disease: the amyloid cascade hypothesis. *Science* **256:** 184–185

Harper JD, Wong SS, Lieber CM, Lansbury PT (1997) Observation of metastable Abeta amyloid protofibrils by atomic force microscopy. *Chem Biol* **4:** 119–125

Hartley DM, Walsh DM, Ye CP, Diehl T, Vasquez S, Vassilev PM, Teplow DB, Selkoe DJ (1999) Protofibrillar intermediates of amyloid beta-protein induce acute electrophysiological changes and progressive neurotoxicity in cortical neurons. *J Neurosci* **19:** 8876–8884

Hepler RW, Grimm KM, Nahas DD, Breese R, Dodson EC, Acton P, Keller PM, Yeager M, Wang H, Shughrue P, Kinney G, Joyce JG (2006) Solution state characterization of amyloid beta-derived diffusible ligands. *Biochemistry* **45:** 15157–15167

IrmingerFinger I, Siegel BD, Leung WC (1999) The functions of breast cancer susceptibility gene 1 (BRCA1) product and its associated proteins. *J Biol Chem* **380:** 117–128

Johansson A-S, Garlind A, Berglind-Dehlin F, Karlsson G, Edwards K, Gellerfors P, Ekholm-Pettersson F, Palmblad J, Lannfelt L (2007) Docosahexaenoic acid stabilizes soluble amyloid-beta protofibrils and sustains amyloid-beta-induced neurotoxicity *in vitro*. *FEBS J* **274:** 990–1000

Kakio A, Nishimoto S, Yanagisawa K, Kozutsumi Y, Matsuzaki K (2002) Interactions of amyloid beta-protein with various gangliosides in raft-like membranes: importance of GM1 ganglioside-bound form as an endogenous seed for Alzheimer amyloid. *Biochemistry* **41:** 7385–7390

Kamenetz F, Tomita T, Hsieh H, Seabrook G, Borchelt D, Iwatsubo T, Sisodia S, Malinow R (2003) APP processing and synaptic function. *Neuron* **37:** 925–937

Kayed R, Head E, Thompson JL, McIntire TM, Milton SC, Cotman CW, Glabe CG (2003) Common structure of soluble amyloid oligomers implies common mechanism of pathogenesis. *Science* **300:** 486–489

Kim SI, Yi JS, Ko YG (2006) Amyloid beta oligomerization is induced by brain lipid rafts. *J Cell Biochem* **99:** 878–889

Klyubin I, Walsh DM, Lemere CA, Cullen WK, Shankar GM, Betts V, Spooner ET, Jiang L, Anwyl R, Selkoe DJ, Rowan MJ (2005) Amyloid beta protein immunotherapy neutralizes Abeta oligomers that disrupt synaptic plasticity *in vivo*. *Nat Med* **11:** 556–561

Lambert MP, Barlow AK, Chromy BA, Edwards C, Freed R, Liosatos M, Morgan TE, Rozovsky I, Trommer B, Viola KL, Wals P, Zhang C, Finch CE, Krafft GA, Klein WL (1998) Diffusible, nonfibrillar ligands derived from Abeta1-42 are potent central nervous system neurotoxins. *Proc Natl Acad Sci USA* **95:** 6448–6453

Lashuel HA, Hartley D, Petre BM, Walz T, Lansbury Jr PT (2002) Neurodegenerative disease: amyloid pores from pathogenic mutations. *Nature* **418:** 291

Lesne S, Koh MT, Kotilinek L, Kayed R, Glabe CG, Yang A, Gallagher M, Ashe KH (2006) A specific amyloid-beta protein assembly in the brain impairs memory. *Nature* **440:** 352–357

Lomas DA, Evans DL, Finch JT, Carrell RW (1992) The mechanism of Z alpha 1-antitrypsin accumulation in the liver. *Nature* **357:** 605–607

McLean CA, Cherny RA, Fraser FW, Fuller SJ, Smith MJ, Beyreuther K, Bush AI, Masters CL (1999) Soluble pool of Abeta amyloid as a determinant of severity of neurodegeneration in Alzheimer's disease. *Ann Neurol* **46:** 860–866

Nilsberth C, Westlind-Danielsson A, Eckman CB, Condron MM, Axelman K, Forsell C, Stenh C, Luthman J, Teplow DB, Younkin SG, Naslund J, Lannfelt L (2001) The 'Arctic' APP mutation (E693G) causes Alzheimer's disease by enhanced Abeta protofibril formation. *Nat Neurosci* **4:** 887–893

O'Nuallain B, Shivaprasad S, Kheterpal I, Wetzel R (2005) Thermodynamics of A beta(1–40) amyloid fibril elongation. *Biochemistry* **44:** 12709–12718

Podlisny MB, Ostaszewski BL, Squazzo SL, Koo EH, Rydell RE, Teplow DB, Selkoe DJ (1995) Aggregation of secreted amyloid beta-protein into sodium dodecyl sulfate-stable oligomers in cell culture. *J Biol Chem* **270:** 9564–9570

Podlisny MB, Walsh DM, Amarante P, Ostaszewski BL, Stimson ER, Maggio JE, Teplow DB, Selkoe DJ (1998) Oligomerization of endogenous and synthetic amyloid beta-protein at nanomolar levels in cell culture and stabilization of monomer by Congo red. *Biochemistry* **37:** 3602–3611

Price JL, Morris JC (1999) Tangles and plaques in nondemented aging and 'preclinical' Alzheimer's disease. *Ann Neurol* **45:** 358–368

Selkoe DJ (1991) The molecular pathology of Alzheimer's disease. *Neuron* **6:** 487–498

Terry RD (2001) Commentary. Copernicus revisited: amyloid beta in Alzheimer disease. *Neurobiol Aging* **22:** 155 discussion 161–153

Townsend M, Shankar GM, Mehta T, Walsh DM, Selkoe DJ (2006) Effects of secreted oligomers of amyloid beta-protein on hippocampal synaptic plasticity: a potent role for trimers. *J Physiol* **572:** 477–492

Walsh DM, Hartley DM, Kusumoto Y, Fezoui Y, Condron MM, Lomakin A, Benedek GB, Selkoe DJ, Teplow DB (1999) Amyloid beta-protein fibrillogenesis. Structure and biological activity of protofibrillar intermediates. *J Biol Chem* **274:** 25945–25952

Walsh DM, Klyubin I, Fadeeva JV, Cullen WK, Anwyl R, Wolfe MS, Rowan MJ, Selkoe DJ (2002a) Naturally secreted oligomers of amyloid beta protein potently inhibit hippocampal long-term potentiation *in vivo*. *Nature* **416:** 535–539

Walsh DM, Klyubin I, Fadeeva JV, Rowan MJ, Selkoe DJ (2002b) Amyloid-beta oligomers: their production, toxicity and therapeutic inhibition. *Biochem Soc Trans* **30:** 552–557

Walsh DM, Lomakin A, Benedek GB, Condron MM, Teplow DB (1997) Amyloid beta-protein fibrillogenesis. Detection of a protofibrillar intermediate. *J Biol Chem* **272:** 22364–22372

Wang W, Hecht MH (2002) Rationally designed mutations convert *de novo* amyloid-like fibrils into monomeric beta-sheet proteins. *Proc Natl Acad Sci USA* **99:** 2760–2765

Wogulis M, Wright S, Cunningham D, Chilcote T, Powell K, Rydel RE (2005) Nucleation-dependent polymerization is an essential component of amyloid-mediated neuronal cell death. *J Neurosci* **25:** 1071–1080

Yip CM, Darabie AA, McLaurin J (2002) Abeta42-peptide assembly on lipid bilayers. *J Mol Biol* **318:** 97–107

Zou K, Kim D, Kakio A, Byun K, Gong JS, Kim J, Kim M, Sawamura N, Nishimoto S, Matsuzaki K, Lee B, Yanagisawa K, Michikawa M (2003) Amyloid beta-protein (Abeta)1-40 protects neurons from damage induced by Abeta1-42 in culture and in rat brain. *J Neurochem* **87:** 609–619